Research Article

Title: Molecular cloning, antiserum preparation and expression analysis during head regeneration of α-crystallin-type heat shock protein in *Hydra vulgaris*

Authors: WEN-FANG DONG, HANG ZHANG, RU-MENG WANG and HONG-CHUN PAN

Address: College of Life science, Anhui Normal University, 1 East Beijing Road, Wuhu 241000, Anhui Province, P. R. China

E-mail: panhongchun@126.com

Running title: Cloning and expression analysis of α-Hsp in *H. vulgaris*

Keywords: *Hydra vulgaris*; α-crystallin-type heat shock protein; polyclonal antiserum; quantitative real-time PCR; whole-mount immunohistochemical assay; RNA interference

Molecular cloning, antiserum preparation and expression analysis during head regeneration of α-crystallin-type heat shock protein in *Hydra vulgaris*[*]

WEN-FANG DONG, HANG ZHANG, RU-MENG WANG and HONG-CHUN PAN[*]

Provincial Key Laboratory of Conservation and Exploitation of Biological Resources in Anhui, Provincial Key Laboratory of Biotic Environment and Ecological Safety in Anhui, College of Life Sciences, Anhui Normal University, Wuhu 241000, Anhui Province, People's Republic of China

Abstract

Our pre-study based on transcriptome profiling indicated that a fragment of α-crystallin-type heat shock protein (α-Hsp) gene was one of numerous cDNA sequences expressed differentially at various stages of head regeneration in *Hydra vulgaris*. In order to further investigate the role which α-Hsp plays during hydra regeneration, a full-length cDNA of *α-Hsp* gene of *H. vulgaris* was isolated by rapid amplification of cDNA ends (RACE) technique in the study. The full-length cDNA of *α-Hsp* gene was 1156 bp, containing a 765 bp open reading frame (ORF) which encodes a polypeptide of 254 amino-acid residues with a molecular weight of 29.27 kDa. Furthermore, the ORF was subcloned into plasmid pET-42a(+), and the recombinant plasmid pET-42a(+)-*α-Hsp* was transformed to *Escherichia coli* BL21(DE3), then the fusion protein GST-α-Hsp was expressed mainly in the form of soluble molecule after induction by IPTG. In addition, BALB/C mice were immunized with the fusion protein to prepare the polyclonal antiserum which was used as primary antibody for whole-mount immunohistochemical assay. The results from immunohistochemical assay showed that α-Hsp had expressed mainly at wound site and nearby area of hydra after decapitation operation, and both quantitative real-time PCR (qPCR) analysis and immunohistochemical assay revealed that the expression level of α-Hsp increased gradually during the early period of hydra regeneration, then reached a peak at 24 hours after decapitation operation, while decreased during the late regeneration period. Moreover, it indicated an important role of *α-Hsp* gene in hydra head regeneration that RNAi-mediated *α-Hsp* silencing led to the obvious delay of the regeneration of head structures in *H. vulgaris*. In conclusion, our results gave the hint that α-Hsp could be related with wound healing and tissue remodeling at early regeneration stages, and may lay the foundation for further study about the physiological function and role of α-Hsp during hydra regeneration.

Introduction

[*]For correspondence. E-mail: panhongchun@126.com

Keywords: *Hydra vulgaris*; α-crystallin-type heat shock protein; polyclonal antiserum; quantitative real-time PCR; whole-mount immunohistochemical assay; RNA interference

The regeneration is a special adaptive capability among many creatures, and it is the process of renewal, restoration, and growth that makes genomes, cells, organisms and ecosystems resilient to natural events that cause damage (Sánchez 2000). Most animals only regenerate the lost or damaged part of its body, while any fragment detached from the bodies of few organisms could regenerate and eventually form one complete body (Birbrair *et al*. 2013). *Hydra* is a genus of freshwater polyp with highly proliferative stem cells in the phylum Cnidaria (Bosch 2007), and if a hydra is cut into two pieces, then each piece can form one fully functional and independent individual (Khalturin *et al*. 2007).

Although the high proportion of stem cells in the body of hydra supports its remarkable regeneration ability, however stem cells is only the material basis, but not determinative factor for its regeneration ability (Bosch 2009). In order to explore the mechanisms underlying hydra regeneration, morphological changes, cell cycle dynamics and related genes during hydra regeneration were studied extensively (Bosch 2007; Galliot 2013; Govindasamy *et al*. 2014; Sun and Irvine 2014), but so far a comprehensive molecular understanding of hydra regeneration is considerable primitive (Gurtner *et al*. 2008; Poss 2010; Li *et al*. 2015; Ninov and Yun 2015; Yun 2015). Luckily, transcriptome, proteome and metabolome studies of hydra may shed much light on the molecular mechanisms controlling regeneration, and preliminary results from some omics data show that hydra regeneration could be an elaborate process that involves complex molecular networks and signal pathways (Lengfeld *et al*. 2009; Wenger et al. 2014; Petersen *et al*. 2015).

Our provious pre-study based on transcriptome profiling indicated that a fragment of *α-Hsp* gene was one of cDNA sequences expressed differentially at various stages of head regeneration in *Hydra vulgaris*. To further investigate the role which α-Hsp plays during hydra regeneration, in the study, the full-length cDNA of *α-Hsp* gene of *H. vulgaris* was cloned by RACE technology according to a transcript-derived fragment, and then polyclonal antiserum was produced by immunizing mice with the recombinant GST-α-Hsp fusion protein which were prepared from a prokaryotic expression system. On the basis of aforementioned works, we determined the expression pattern of α-Hsp during hydra head regeneration by qPCR analysis and whole-mount immunohistochemical assay, and provide a foundation for studying the function of α-Hsp in hydra.

Materials and methods

Animals and treatment

H. vulgaris was collected from Anqin in China, and cultured with a medium (1 mM $CaCl_2$, 0.1 mM KCl, 0.1 mM $MgCl_2$, and 0.5 mM NaH_2PO_4, pH7.6) in an illumination incubator under a 12L:12D photoperiod (light intensity of 300 μmol m^{-2} s^{-1}) at 20 ± 0.5 °C. The animals were fed daily with the nauplii of *Artemia salina*, and were transferred to fresh culture medium 0.5 h after each feeding. Prior to RNA extraction, 20 individuals of *H. vulgaris* were snap-frozen in liquid nitrogen and stored at -80 °C.

RNA extraction and cDNA synthesis

Total RNA was isolated from *H. vulgaris*, using a Trizol Kit (Sangon, Shanghai, China) following the manufacturer's instructions. The concentration and quality of the extracted total RNA were

checked by agarose gel electrophoresis and measured by HY1600 Portable Spectrophotometer (Anytester, Hefei, China). cDNA library was constructed with SMART™ RACE cDNA Amplification Kit (TaKaRa Bio, Otsu, Japan) according to user manual.

Cloning of α-Hsp gene

The gene-specific primers 5' Hsp and 3' Hsp (table 1) were designed and synthesized according to the *α-Hsp* unigenes in our previous transcriptome data of *H. vulgaris*. With the primer 5' Hsp and 5' adapter primer (table 1) as primer pairs, the 5'-RACE was carried out in a total volume of 50 μL, containing 2 μL ready cDNA library, and performed under the conditions: 94 °C for 5 min followed by 35 cycles of amplification (94 °C for 30 s, 52 °C for 30 s, 72 °C for 1 min). In addition, The 3'-RACE was performed with the primer 3' Hsp and 3' adapter primer (table 1) in a total volume of 50 μL containing 2 μL ready cDNA library under the conditions: 94 °C for 5 min followed by 35 cycles of amplification (94 °C for 30 s, 56 °C for 30 s, 72 °C for 1 min). These PCR products were purified, subcloned into pMD-18T vector (TaKaRa Bio, Otsu, Japan) and sequenced. Whereafter, the full-length cDNA sequence of *α-Hsp* gene was obtained by PCR with primers Hsp-F and Hsp-R (table 1) which were designed according to the 5' and 3' sequences of *α-Hsp* gene from RACE. 2 μL ready cDNA library was used for the PCR in a total volume of 50 μL under the conditions: 94 °C for 5 min followed by 35 cycles of amplification (94 °C for 30 s, 58 °C for 30 s, 72 °C for 1 min), then the PCR product was also purified and subcloned into pMD-18T vector (TaKaRa Bio, Otsu, Japan) to form the recombinant plasmid pMD-18T-*α-Hsp* which was extracted with Plasmid Purification Kit (Sangon, Shanghai, China) and sequenced.

Insert Table 1

Bioinformatics analysis

Clustal software (Version 2.0) was used for multiple alignments of protein (amino acid) or DNA (nucleic acid) sequences (Sievers and Higgins 2014). Protein primary, secondary and tertiary structure analysis were performed respectively online at the websites http://www.proteomics.com.cn/tools/mwcal/, http://nhjy.hzau.edu.cn/kech/swxxx/jakj/Expasy and http://swissmodel.expasy.org/interactive (Bienert *et al*. 2017), and AntheProt_3D was used for 3-D model display. In addition, ProtTest 2.4 was used to identify the optimal evolutionary model for protein sequence alignments (Abascal *et al*. 2005), then phylogenetic tree was reconstructed by maximum likelihood estimation method with PAUP 4.0b10 software and the reliability of each node was established by bootstrap methods (Jeon *et al*. 2016).

Prokaryotic expression, purification and Confirmation of recombinant α-Hsp

With PE-Hsp-F and PE-Hsp-R (table 1) as primer pairs, the ORF of *α-Hsp* gene was amplified with the ready plasmid pMD-18T-*α-Hsp* as template, and the PCR reaction was performed using PrimeSTAR HS DNA Polymerase Kit (TaKaRa Bio, Otsu, Japan). The PCR product was cut with *Nco* I and *Xho* I, purified and subcloned in a similarly digested plasmid pET-42a(+) (Invitrogen, Carlsbad, USA) to form the recombinant plasmid pET-42a(+)-*α-Hsp* carrying a 6× His-tag and a GST-tag at the N-terminal. *E. coli* BL21(DE3) transformed with pET-42a(+)-*α-Hsp* was grown in liquid LB medium containing 100 mg/L kanamycin at 32 °C, with agitation (250 rpm), until it reached an OD of about 0.6. The cells were then induced by addition of 1 mM IPTG

(isopropyl-β-D-thiogalactopyranoside) and cultivated for a further 4 h for the target protein expression. The total bacterial proteins were extracted using Bacterial Protein Extraction Kit (Sangon, Shanghai, China) and the recombinant GST-α-Hsp fusion protein was purified with the 6× His-Tagged Protein Purification Kit (Sangon, Shanghai, China). The prepared protein samples were then loaded onto a 13% SDS-PAGE and separated on a Mini-Protean Tetra (Bio-Rad Laboratories, Hercules, USA). Furthermore, the concentration of the purified protein was determined by Bradford's method (Gasparov and Degtiar' 1994).

MALDI-TOF-MS (Matrix-Assisted Laser Desorption / Ionization Time of Flight Mass Spectrometry) peptide mapping method was used for the confirmation of the recombinant protein (Egelhofer *et al*. 2002). The purified protein band was manually excised from SDS-PAGE gel, washed with Milli-Q water for three times, destained with 100 mM NH_4HCO_3, dried twice with 100% acetonitrile, and digested overnight at 37 °C with 10 ng/μl trypsin (Promega, Madison, USA) in 50 mM NH_4HCO_3. The peptides were extracted twice with 0.1% TFA in 50% acetonitrile, and the extracts were pooled and lyophilized. The resulting lyophilized tryptic peptides were dissolved in 5mg/ml hydroxy-cinnamic acid containing 0.1% trifluoroacetic acid and 50% acetonitrile. MALDI-TOF-MS analysis were conducted with AB 4800 MALDI-TOF-TOF instrument (Applied Biosystems, Newyork, USA). All spectra were submitted to database searching using online MASCOT program (http://www.matrixscience.com).

Preparation of polyclonal antiserum against GST-α-Hsp fusion protein

According to previously description (Koolivand *et al*. 2016), polyclonal antiserum was prepared in five BALB/C mice (20 to 25 g) using the purified recombinant GST-α-Hsp fusion protein as antigen, and these animals were immunized four times at two weeks interval. The first abdominal injection was done with the mixture of antigen protein and complete Freund's adjuvant (1:1, v/v), and other three remaining injections with the mixture of antigen protein and incomplete Freund's adjuvant (1:1, v/v). Bleedings were carried out two weeks after the last injection, and blood samples were allowed to coagulate for 2 h at 37 °C and 1 h at 4 °C, then centrifuged at 3,000 g for 15 min at 4 °C. The supernatant (antiserum) was stored at -80 °C. Furthermore, the titer of the antiserum was measured by indirect ELISA (enzyme-linked immunosorbent assay) method with ELISA Kit (Shanghai Elisa Biotech Inc., Shanghai, China).

Hydra Regeneration Experiments

Regeneration experiments were carried out with 48 h starved, budless individuals of *H. vulgaris*. First batches of three hundred animals were decapitated at 80% body length (figure 1), transferred into fresh medium, and allowed to regenerate in a dark incubator at 20 ± 0.5 °C. In order to prepare for qPCR, ten animals were dissolved with Trizol solution (Sangon, Shanghai, China) in a 1.5 ml sterile eppendorf tube respectively at 0, 8, 16, 24, 32, 40, 48, 56, 64 and 72 h after decapitation operation, and three biological replicates were prepared for each time point. In addition, second batches of one hundred animals were also decapitated and allowed to regenerate as above, then ten animals were fixed with 4% phosphate-buffered paraformaldehyde in an incubator chamber (4 °C) respectively at 0, 8, 16, 24, 32, 40, 48, 56, 64 and 72 h after decapitation operation for whole-mount immunohistochemical assay.

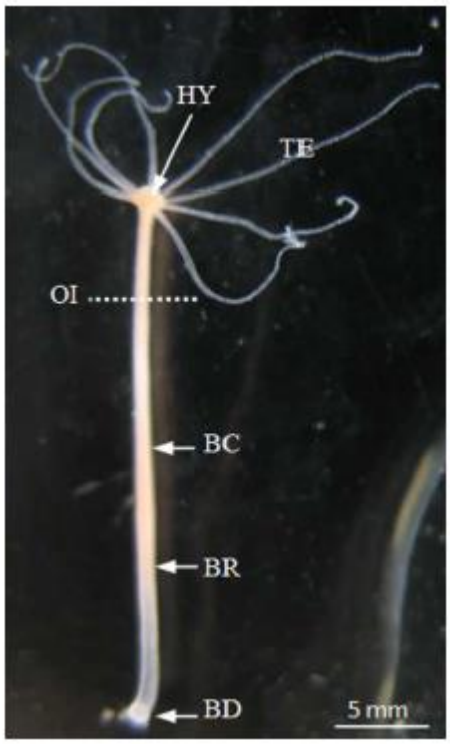

Figure 1. The configuration of *H. vulgaris*. BC, body column; BD, basal disc; BR, budding region; HY, hypostome; OI, operative incision; TE, tentacle

Quantitative real-time PCR

To evaluate expression level of *α-Hsp* gene during hydra head regeneration, qPCR was performed with CFX96 Touch Real-Time PCR Detection System (Bio-Rad Laboratories, Hercules, USA) and SYBR® Premix Ex Taq™ (Tli RNaseH Plus) kit (TaKaRa Bio, Otsu, Japan). Total RNA was isolated with a Trizol kit (Sangon, Shanghai, China) following the manufacturer's instructions. First-strand cDNA synthesis was performed with 1 μg total RNA by PrimeScript™ 1st Strand cDNA Synthesis Kit (TaKaRa Bio, Otsu, Japan). Each qPCR reaction solution contained 2 μL of cDNA, 12.5 μL of SYBR Premix Ex Taq（Tli RNaseH Plus）(TaKaRa Bio, Otsu, Japan), 0.5 μL of each primer (Q-Hsp-F and Q-Hsp-R, table 1) and 9.5 μL nuclease-free PCR-grade water. In particular, the constitutively expressed *actin* gene in *H. vulgaris*, amplified with the primers Q-Actin-F and Q-Actin-R (table 1), was used as an internal control to normalize the relative expression level of the analysed *α-Hsp* gene in *H. vulgaris*. qPCR was performed under the conditions: 95 °C for 3 min followed by 40 cycles of amplification (95 °C for 30 s, 60 °C for 30 s). Each sample was experimented in triplicate. Finally, the qPCR data were analysed according to the comparative Ct method (Ali-Benali *et al*. 2005).

Whole-mount immunohistochemical assay

Whole-mount immunohistochemical assay for α-Hsp in *H. vulgaris* was carried out according to a

modified method based on previous descriptions (White and Sillitoe 2013). After initial fixation within 4% phosphate-buffered paraformaldehyde mentioned earlier in the paper, hydra samples were postfixed in Dent's fixative (4 parts anhydrous methanol and 1 part dimethysulfoxide (DMSO)) overnight at 4 °C, and the next day incubated in Dent's bleach (4 parts anhydrous methanol, 1 part DMSO and 1 part 30% hydrogen peroxide (H_2O_2)) for 2 h to block endogenous peroxidase activity. Subsequently, hydra samples were dehydrated twice in anhydrous methanol for 30 min each and subjected to four cycles of freezing in anhydrous methanol and thawing to room temperature (RT), and then incubated overnight in anhydrous methanol at -80 °C.

The following day hydra samples were rehydrated for 1 h each in 50% and 15% methanol in PBS at RT, and then enzymatically digested in 10 μg/ml proteinase K for 5 min at RT. After being rinsed three times for 15 min in PBS at RT and blocked by incubating in PBSMT (2% non-fat skim milk powder, 0.1% Triton X-100 in PBS) (Davis, 1993) for 8 h, hydra samples were incubated in the antiserum against GST-α-Hsp which was diluted in PBSMT containing 5% DMSO for 24 h at 4 °C. After this incubation, hydra samples were washed in PBSMT three times for 1 h each and then incubated overnight in secondary antibodies (Goat Anti-Mouse IgG Fc-HRP) (AmyJet Scientific Inc, Wuhan, China) diluted in PBSMT containing 5% DMSO at 4 °C. After the treatment of secondary antibodies, hydra samples were washed three times in PBSMT for 1 h each and then incubated in PBSMT overnight to ensure removal of unbound antibodies.

Before the staining reaction, hydra samples were rinsed with 0.1% Triton X-100 in PBS (PBT) (Davis, 1993) for 2 h at RT. The staining reaction solution, consisting of 10 mg ABTS (2, 2'-azino-bis(3-ethylbenzothiazoline-6-sulfonic acid), 10 μL 30% H_2O_2 and 20 ml PBT, should be prepared freshly. Hydra samples were incubated in the staining reaction solution for 20 min, and then washed in PBT three times for 2 min each, in the end incubated in 2% NaF until nonspecific background staining was as light as possible. Photomicrographs of hydra samples were captured with a SteREO Discovery.V20 stereomicroscope (Carl Zeiss, Hamburg, Germany).

Design, Synthesis and screening of candidate siRNA sequences for α-Hsp gene silencing

According to *α-Hsp* gene cDNA sequence of *H. vulgaris* obtained in the study, five candidate siRNA sequences for *α-Hsp* gene silencing (table 2) were designed with DSIR online software (http://biodev.extra.cea.fr/DSIR/DSIR.html) (Vert *et al*. 2006) and siDirect 2.0 online software (http://sidirect2.rnai.jp/) (Naito *et al*. 2009), and synthesized by Shanghai Sangon Company (Shanghai, China). In addition, a random siRNA sequence was synthesized and used as a nonspecific control.

In order to select the effective siRNA sequences from five candidate siRNA sequences (table 2), RNA interference (RNAi) experiments were carried out with 48 h starved, budless individuals of *H. vulgaris*. For one of these five candidate siRNA sequences, 24 animals about 1 cm in height were placed in individual wells of a 24-well plate (Sangon, Shanghai, China) with 100 μL of sterile medium (1 mM $CaCl_2$, 0.1 mM KCl, 0.1 mM $MgCl_2$, and 0.5 mM NaH_2PO_4, pH7.6). The liposomal compound 1,2-dimyristyloxypropyl-3-dimethyl-hydroxy ethyl ammonium bromide linked to cholesterol (DMRIE-C; Invitrogen, Carlsbad, USA) was used as an RNA transfection agent (Dunn *et al*. 2007; Ochiya *et al*. 1999; Valentina *et al*. 1995). Once the animals had reacclimatized, the sterile medium was removed and replaced with 100 μL of sterile medium containing dsRNA (75 μg per 100 μL medium) and DMRIE-C (0.3 μL per 100 μL medium). After 48 h, all animals were decapitated at 80% body length (figure 1), transferred into fresh medium,

and allowed to regenerate in a dark incubator at 20 ± 0.5 °C. In order to prepare for qPCR, eight animals were dissolved with Trizol solution (Sangon, Shanghai, China) in a 1.5 ml sterile eppendorf tube at 24 h after decapitation operation, and three biological replicates were prepared for the trial. Total RNA was isolated with a Trizol kit (Sangon, Shanghai, China) following the manufacturer's instructions. First-strand cDNA synthesis was performed with 1 μg total RNA by PrimeScript™ 1st Strand cDNA Synthesis Kit (TaKaRa Bio, Otsu, Japan). Each qPCR reaction solution contained 2 μL of cDNA, 12.5 μL of SYBR Premix Ex Taq（Tli RNaseH Plus）(TaKaRa Bio, Otsu, Japan), 0.5 μL of each primer (Q-Hsp-F and Q-Hsp-R, table 1) and 9.5 μL nuclease-free PCR-grade water. In addition, *actin* gene in *H. vulgaris*, amplified with the primers Q-Actin-F and Q-Actin-R (table 1), was used as an internal control to normalize the relative expression level of the analysed *α-Hsp* gene in *H. vulgaris*. qPCR was performed under the conditions: 95 °C for 3 min followed by 40 cycles of amplification (95 °C for 30 s, 60 °C for 30 s). Then, the qPCR data were analysed according to the comparative Ct method (Ali-Benali *et al*. 2005).

The effect of α-Hsp gene silencing on the process of hydra head regeneration

To examine the influence of *α-Hsp* RNAi on head regeneration, RNA interference (RNAi) experiments were carried out with 48 h starved, budless individuals of *H. vulgaris*. First batches of 96 animals about 1 cm in height were used for RNAi experiments based on the most effective one of five candidate siRNA sequences (table 2). These polyps were placed in individual wells of a 96-well plate (Sangon, Shanghai, China) with 100 μL of sterile medium. The liposomal compound DMRIE-C (Invitrogen, Carlsbad, USA) was used as an RNA transfection agent. Once the animals had reacclimatized, the sterile medium was removed and replaced with 100 μL of sterile medium containing dsRNA (75 μg per 100 μL medium) and DMRIE-C (0.3 μL per 100 μL medium). After 48 h, all animals were decapitated at 80% body length (figure 1), transferred into fresh medium, and allowed to regenerate in a dark incubator at 20 ± 0.5 °C. Then, the 96 polyps were observed and photographed one by one under a SteREO Discovery.V20 stereomicroscope (Carl Zeiss, Hamburg, Germany) respectively at 40, 48, 56 and 64 h after decapitation operation for recording regeneration process. In addition, another batches of 96 animals about 1 cm in height were used for control experiments based on a random siRNA sequences.

Statistical treatment of results

The Statistical Package for the Social Sciences (SPSS) (ver. 20.0) was used for gene expression analysis from qPCR, and all the results are expressed as mean ± SE. Differences within a group data were compared using one-way analysis of variance and the Student–Newman–Keuls post hoc test, while differences between groups were compared using the paired samples t-test. Additionally, significance was set at $P < 0.05$ and $P < 0.01$ in two-tailed testing.

Results

Cloning and characterization of α-Hsp gene in H. vulgaris

Based on the sequence of *α-Hsp* gene fragment in the transcriptome of *H. vulgaris*, the cDNA sequence of *α-Hsp* in *H. vulgaris* was cloned by RACE technology (figure 2). The full-length cDNA of *α-Hsp* gene was 1156 bp and contained an open reading frame (ORF) of 765 bp (figure 3), flanked by stretches of 200 and 191 bp at the 5'-untranslated and 3'-untranslated regions,

respectively. The resulting sequence was deposited into GenBank with accession number KU981065, and the deduced protein encoded 254 amino acid residues with a calculated molecular mass of 29.27 kDa and a theoretical isoelectric point (pI) of 6.43. In addition, the conserved domain prediction of NCBI database showed that the deduced protein in *H. vulgaris* belonged to α-Hsp superfamily, and it had two α-crystallin domains (figure 3) which share 41.18% sequence identity (figure 4).

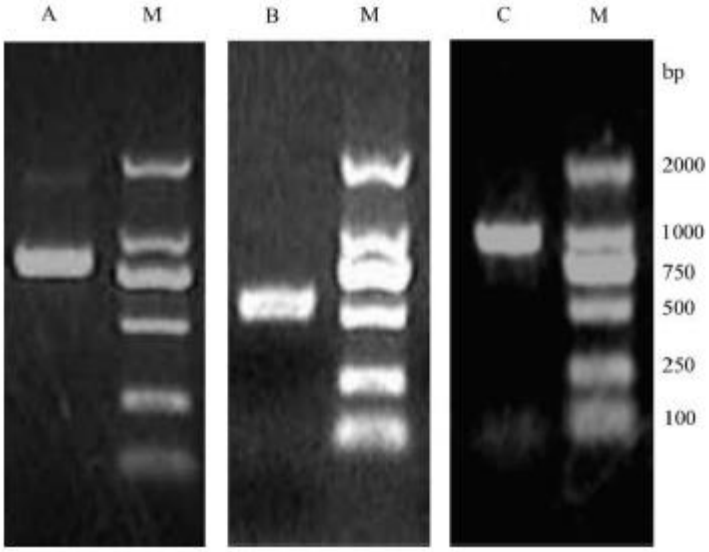

Figure 2. Agarose gel electrophoresis of PCR amplification of *α-Hsp* gene. Lane A, 3' RACE PCR fragments; Lane B, 5' RACE PCR fragments; Lane C, full-length cDNA of *α-Hsp* gene; Lane M, molecule weight marker of DNA.

Figure 3. The full-length cDNA and deduced amino acid sequences of α-Hsp from *H. vulgaris*. The start codon (ATG) is in red, and stop codon (TGA) is in green. Domain 1 is highlighted in blue, and domain 2 is highlighted in purple.

Figure 4. Alignment result of deduced amino acid sequences of domain 1 and domain 2 in α-Hsp from *H. vulgaris*.

Structure predication of α-Hsp

The prediction of secondary structure indicated that the deduced α-Hsp from *H. vulgaris* consisted of random coils (51.18%), α-helices (17.72%), β-sheets (23.62%) and β-turns (7.48%) (figure 5). According to the appropriate modeling model 2bol.1.A which was screened out online at http://swissmodel.expasy.org/interactive based on amino acid sequence of α-Hsp from *H. vulgaris*, its three-dimensional structure was predicted by homology modeling method (figure 6). Its two conserved domains formed severally a relatively independent structure, each of which had a "cylindrical cage" core that was made of several β-sheets (figure 6).

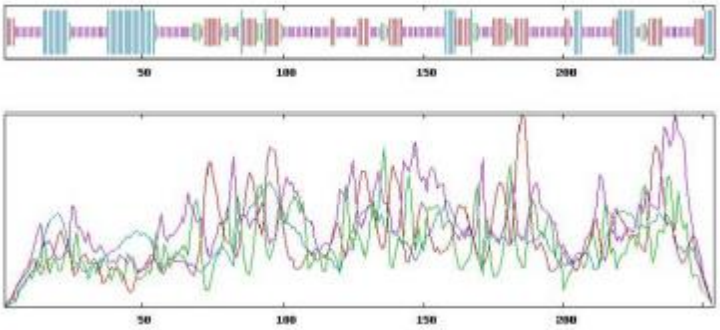

Figure 5. The deduced secondary structure of α-Hsp from *H. vulgaris*. α-Helices, β-sheets, β-turns and random coils are indicated with blue, red, green and pink lines respectively.

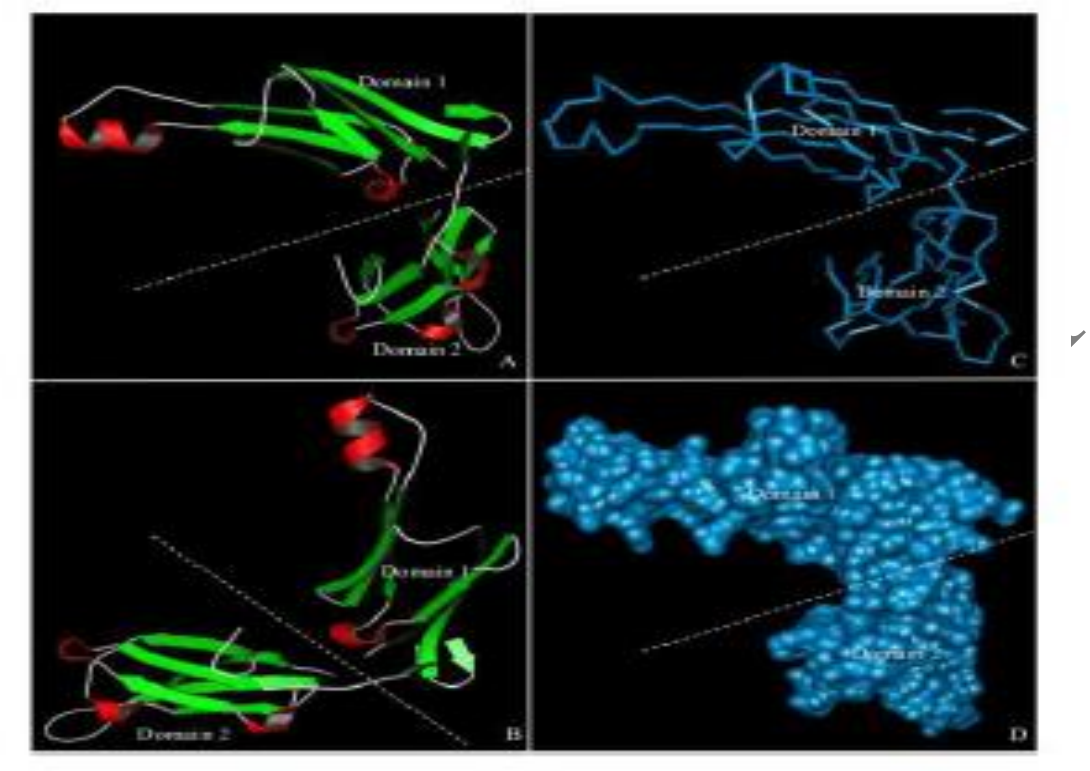

Figure 6. The deduced 3-D structure of α-Hsp from *H. vulgaris*. A, the predicted three-dimensional structure. Red helices represent α-helix, green arrows represent β-sheet, and white filaments represent random coils; B, figure A was rotated 90 degrees clockwise; C, alpha trace; D, surface structure.

Phylogenetic tree depicting the relationships among α-Hsp domains

The results of Blastp analysis about two conserved domains of α-Hsp from *H. vulgaris* in NCBI indicated that there were many homologous sequences from vertebrate groups, while few from invertebrate groups. In order to investigate the evolutionary relationship among α-crystallin domains from different species, a phylogenetic tree was reconstructed based on 25 α-crystallin domains with two homologous sequences from bacteria as outgroup (figure 7). In the tree, the relationship among different animal groups is roughly identical to that among them based on morphological evidences, and the cnidaria group, which contained *H. vulgaris* and one sea anemone (*Nematostella vectensis*), was located at the root of the phylogenetic tree.

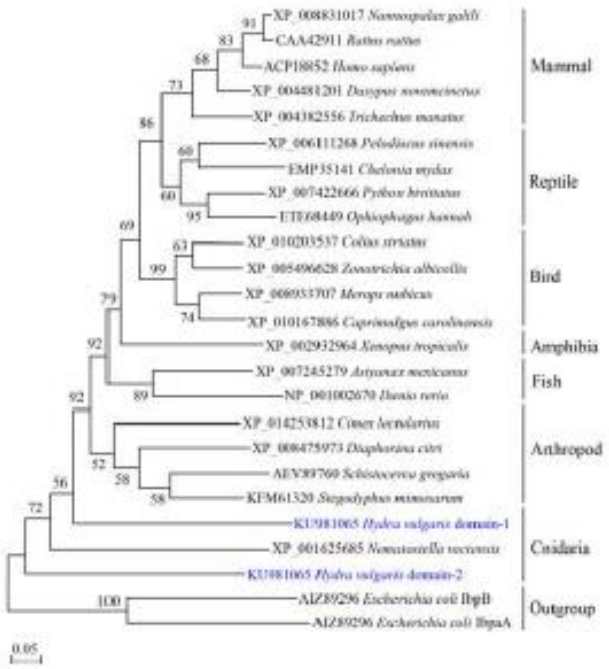

Figure 7. Maximum likelihood tree based on amino acid sequences of α-Hsp domains from different species. The tree was reconstructed under the LG+G+I+F model estimated by ProtTest 2.4, and the nodal numbers are bootstrap values from maximum likelihood analysis of the 1000 bootstrap replications. The domains from *H. vulgaris* were highlighted in blue.

Prokaryotic expression of α-Hsp and preparation of polyclonal antiserum

After ligation of the ORF of *α-Hsp* gene from *H. vulgaris* into prokaryotic expression vector pET-42a(+), the recombinant vector pET-42a(+)-*α-Hsp* was identified by restriction enzyme digestion (figure 8) and nucleotide sequencing, then transformed into *E. coli* strain BL21 (DE3). The expressing cells were harvested at the 4th hour after induction with IPTG, and the expression of the recombinant GST-α-Hsp fusion protein was proved on 13% SDS-PAGE by an intense band of which the molecular weight (MW) corresponded roughly to the predicted MW (about 62.14 kDa) of ORF amino acids of α-Hsp plus all the fused amino acid tags (figure 9), and further comfirmed by peptide mass fingerprinting (PMF) based on MALDI-TOF-MS peptide mapping analysis.

In addition, SDS-PAGE result also showed that the recombinant protein existed mainly in the form of soluble molecule (figure 9). The concentration of the purified fusion protein GST-α-Hsp by affinity chromatography was estimated to be about 350 μg/ml, so it was used appropriately as antigen to immunize mice. After five mouse were immunized by fusion protein GST-α-Hsp, the derived antiserum was titrated by the use of ELISA with different dilutions in the range of 1:500 to 1: 29524,500, then the ELISA results revealed that the titer of the antiserum against GST-α-Hsp was about 1: 3280,500 (figure 10).

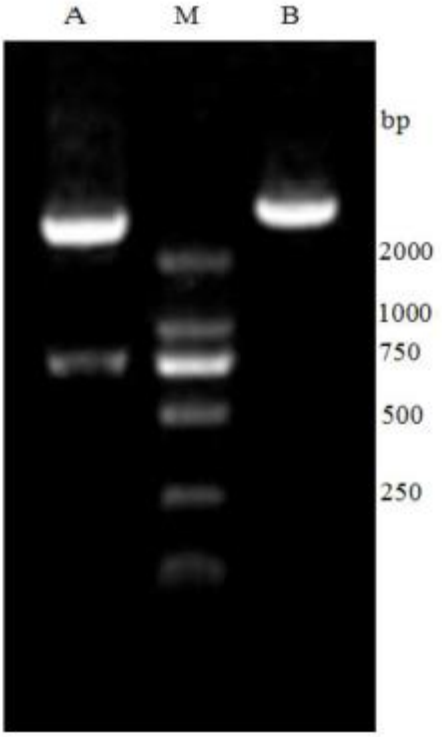

Figure 8. Identification of recombinant vector pET42a(+)-*α-Hsp*. Lane A, the recombinant vector pET42a(+)-*α-Hsp* was digested by both *Nco* I and *Xho* I; Lane M, molecule weight marker of DNA; Lane B, the recombinant vector pET42a(+)-*α-Hsp* was digested by *Nco* I .

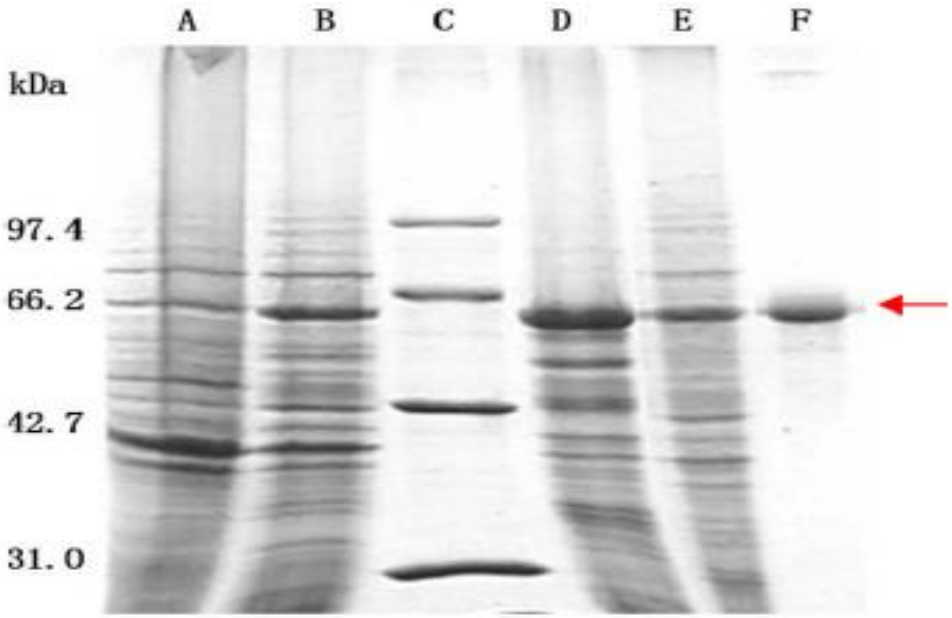

Figure 9. SDS-PAGE of recombinant GST-α-Hsp fusion protein. Lane A, the total proteins from uninduced *E. coli* BL21(DE3) harbouring pET42a(+)-*α-Hsp*; Lane B, the total proteins from induced *E. coli* BL21(DE3) harbouring pET42a(+)-*α-Hsp*; Lane C, molecule weight marker of protein; Lane D, the soluble cell fraction from induced *E. coli* BL21(DE3) harbouring pET42a(+)-*α-Hsp* after sonic treatment; Lane E, the insoluble cell fraction from induced *E. coli* BL21(DE3) harbouring pET42a(+)-*α-Hsp* after sonic treatment; Lane F, the recombinant GST-α-Hsp fusion protein purified via His-tag affinity chromatography (Ni-NTA His-Bind Resin).

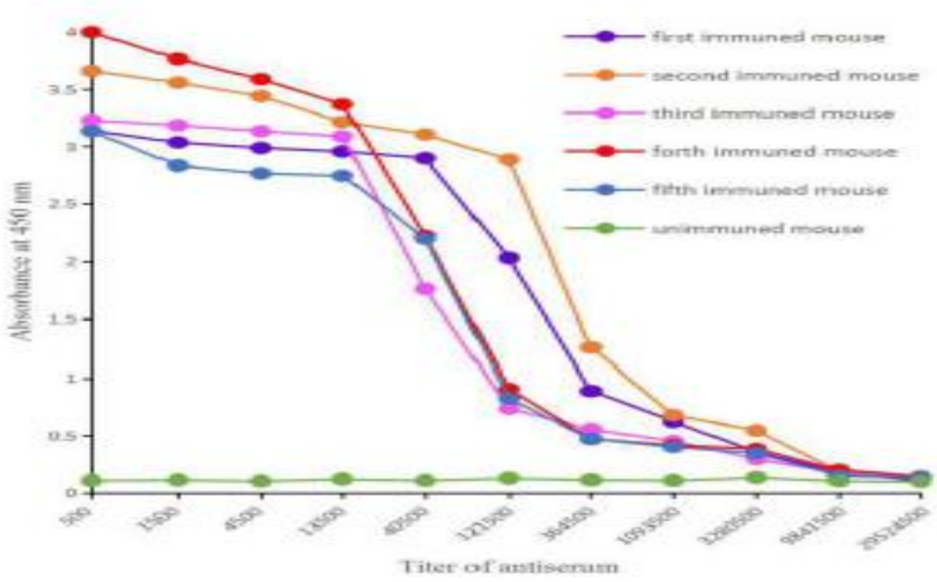

Figure 10. Titration of antiserum to GST-α-Hsp fusion protein using indirect enzyme-linked immunosorbent assay (ELISA). The graph is based on absorbance values of the wells treated with different dilutions of the antiserum.

Expression analysis of α-Hsp during hydra head regeneration

qPCR analysis was performed to reveal the expression pattern of *α-Hsp* gene at different stages during hydra head regeneration (figure 2). The results indicated that the transcript levels of *α-Hsp* gradually increased from 0 h to 24 h after decapitation operation, and then reached a peak at 24 h. While after 24 h, the transcript level of *α-Hsp* was down-regulated by degrees, and its transcript level at late stages of regeneration (48 h, 56 h and 64 h after decapitation operation) was very close to that at 0 h (figure 11).

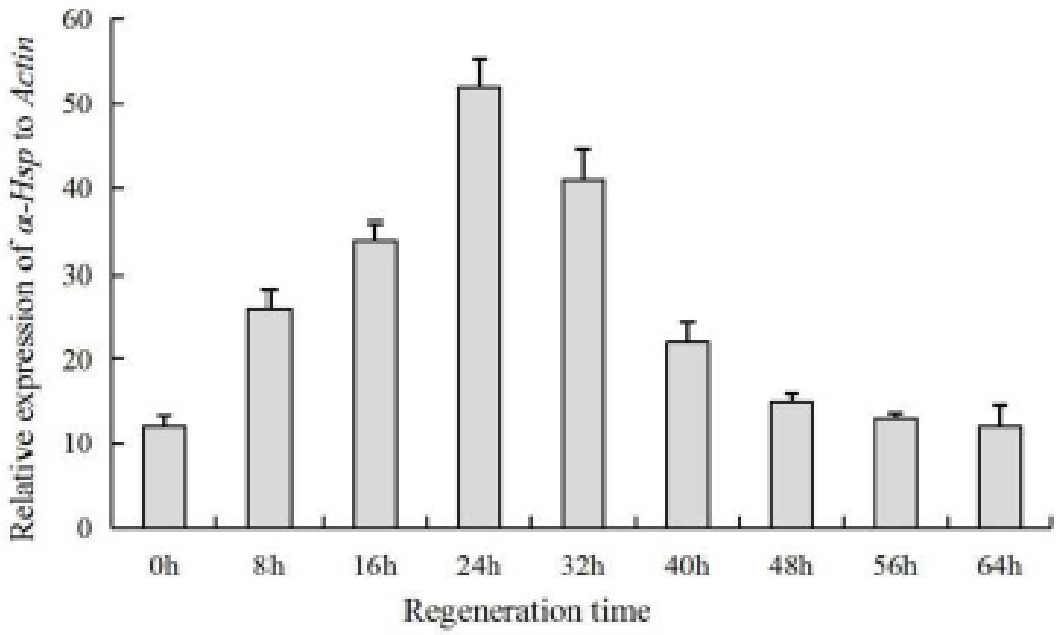

Figure 11. Relative expression levels of *α-Hsp* gene of *H. vulgaris* at different regeneration stages. The Actin gene was used as a control to normalize the transcript level. Error bars exhibit the standard deviation of triplicate experiments.

In order to explore the temporal and spatial expression patterns of α-Hsp protein, the whole-mount immunohistochemical assay was used in the study. The immunohistochemical results showed that α-Hsp was expressed mainly at the wound site and nearby area of hydra (figure 12B-F), and could be detectable at 8 h after decapitation operation. Subsequently, α-Hsp expression increased gradually (figure 12B-D), while started to decline at 32 h after decapitation operation (figure 12D-F), and was barely visible at 40 h after decapitation operation (figure 12F-I).

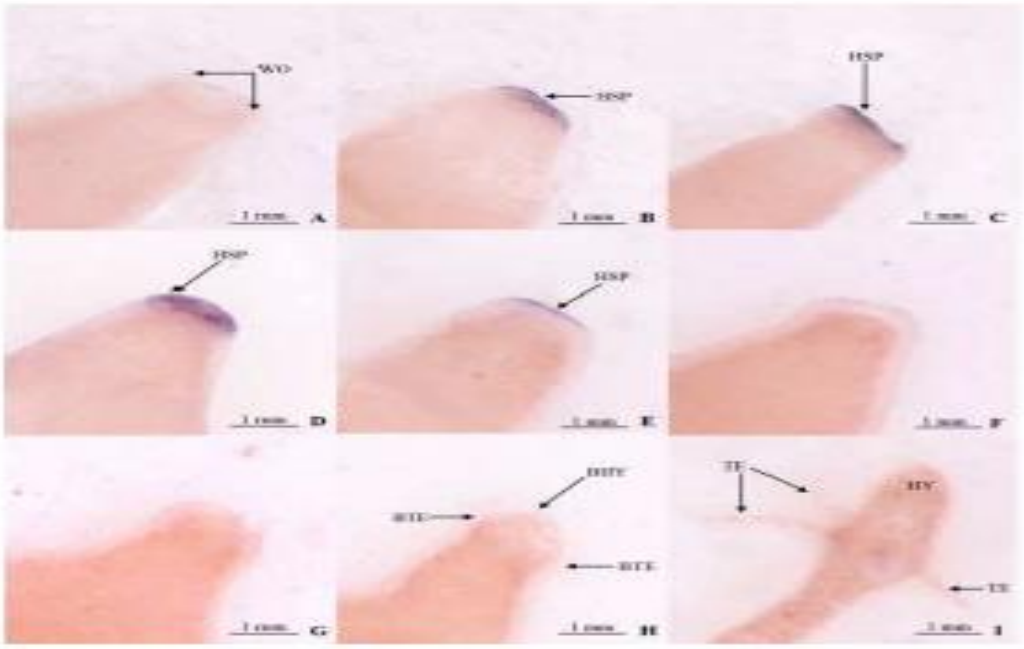

Figure 12. α-Hsp protein expression analysis during hydra head regeneration in *H. vulgaris* based on whole-mount immunohistochemical assay. A, the wound region at 0 h after operation; B, the wound region at 8 h after operation; C, the wound region at 16 h after operation; D, the wound region at 24 h after operation; E, the wound region at 32 h after operation; F, the wound region at 40 h after operation; G, the wound region at 48 h after operation; H, the wound region at 56 h after operation; I, the wound region at 64 h after operation; BHY, bud of new hypostome; BTE, bud of new tentacle; HSP, the expression region of α-Hsp (fuchsia region); HY, hypostome; TE, tentacle; WO, wound

α-Hsp gene silencing led to the obvious delay of the regeneration of head structures in H. vulgaris

According to the above results that the expression level of *α-Hsp* in *H. vulgaris w*as highest at 24 hours after decapitation operation (figure 11, figure 12), relative expression levels of *α-Hsp* gene of siRNA-treated polyps at 24 h after decapitation operation were measured by qPCR to assess the efficiency of RNAi-mediated *α-Hsp* silencing. qPCR results indicated that *α-Hsp* transcript level of trial group treated by Hsp-siRNA-3 (table 2) was lower than that of trial groups treated by other four candidate siRNA sequences (figure 13), then Hsp-siRNA-3 was used for RNAi experiment in order to study the effect of α-Hsp gene silencing on the process of hydra regeneration. Compared with control group treated by random siRNA, trial group treated by Hsp-siRNA-3 had a significantly reduced capacity for head regeneration (figure 14). At 64 h after decapitation operation, as shown in figure 14, only about 9% (n = 96) of polyps treated by Hsp-siRNA-3 had a fully developed head, while up to 75% (n = 96) in control group. Moreover, 54% (n = 96) of

polyps treated by Hsp-siRNA-3 had failed to regenerate any head structures compared to none in control group. In a word, *α-Hsp* gene silencing led to the obvious delay of the regeneration of head structures in *H. vulgaris*.

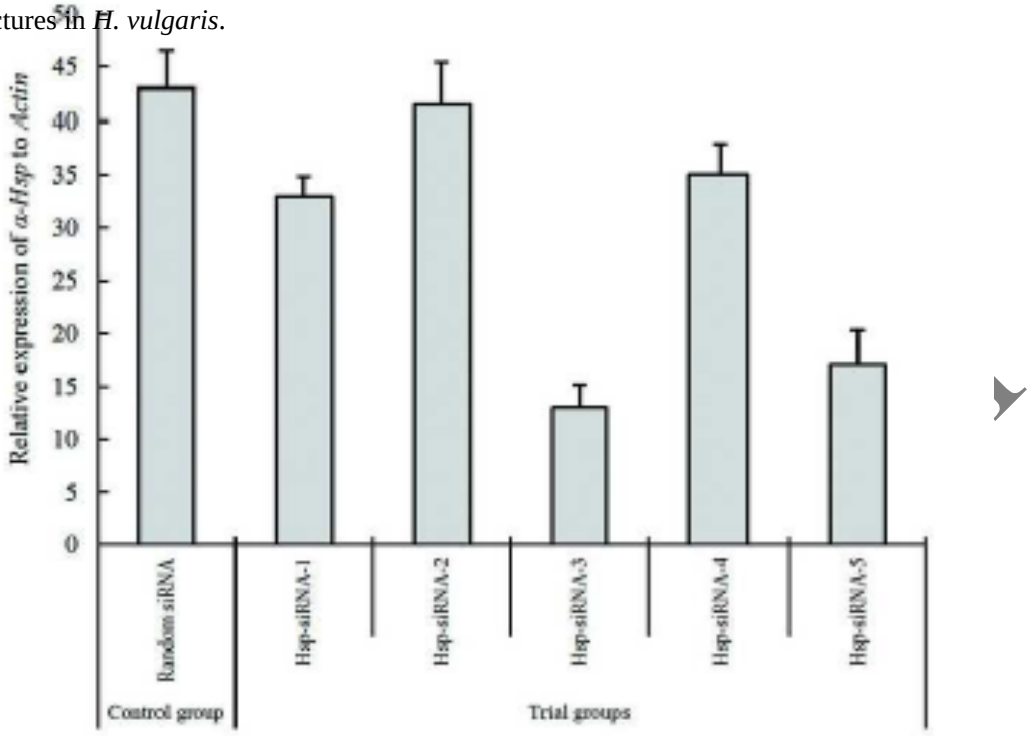

Figure 13. Relative expression levels of *α-Hsp* gene of polyps at 24 h after decapitation operation, measured by qPCR. These polyps were treated with candidate siRNA for silencing *α-Hsp* gene (trial group) or random siRNA (control group) before decapitation operation. The *Actin* gene was used as a control to normalize the transcript level. Error bars exhibit the standard deviation of triplicate experiments.

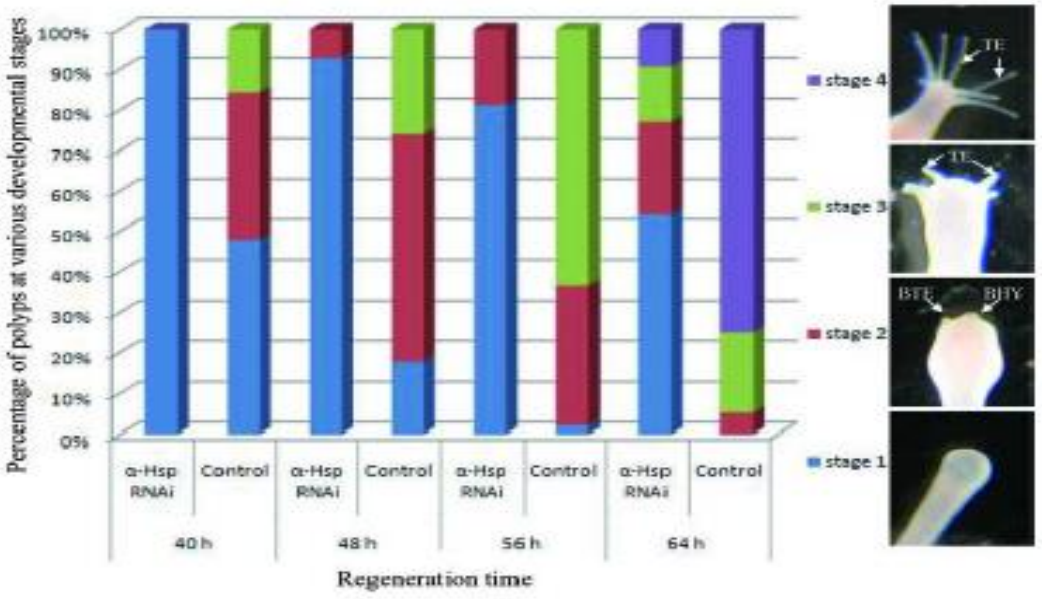

Figure 14. The percentage of polyps of the various developmental stages during head regeneration. Histogram showed that *α-Hsp* RNAi caused an obvious delay in the regeneration of head structures, and photographs showed different morphological stages of head regeneration in *H. vulgaris*. Stage 1, having no tentacles; stage 2, having a tentacle bud that first appeared; stage 3, having less than five short tentacles which were still immature; stage 4, having more than five long tentacles which were already mature. BHY, bud of new hypostome; BTE, bud of new tentacle; TE, tentacle.

Discussion

The crystalline lens in the vertebrate eye is a transparent, biconvex structure that helps to refract light to be focused on the retina along with the cornea, and it consists mainly of long, thin and transparent cells (Bloemendal *et al*. 2004). Within the mature lens cells (also known as lens fiber), the absence of light-scattering organelles (such as the mitochondria, endoplasmic reticulum and nucleus) and the filling of crystallins which tend to form soluble, high-molecular weight aggregates increasing the index of refraction of the lens are the key factors for maintaining the transparency of the lens (Hoehenwarter *et al*. 2006). Furthermore, there are three main crystallin types in the vertebrate lens: α-, β-, and γ-crystallins. β- and γ- crystallins are found primarily in the lens, while subunits of α-crystallin have also been detectable in other parts of the eye and the body (Andley 2006). It is no doubt that α-crystallin functions as structure protein in lens, but what role does α-crystallin play in other tissues except with lens? It was not until when *Drosophila* small heat-shock proteins (sHsps) were found to share conspicuous sequence similarities with α-crystallin that the question was answered (Ingolia and Craig 1982), since then α-crystallin was referred to as α-crystallin-type heat shock protein (α-Hsp).

Follow-up researches indicated that α-Hsp was found in small amounts in many other mammalian tissues and in many (but not all) bacteria, animals, and plants, as well as in some representatives of archaea (de Jong *et al*. 1998), and the most important role of α-Hsp is as a molecular chaperone which makes some target proteins fold properly by combining with them or helps intracellular damaged proteins under stress to refold for preventing them from denaturing or inactivating (MacRae 2000). And, more remarkable, members of the α-Hsp superfamily are characterized by the presence of a homologous sequence of about 80-100 amino acid residues, a so-called α-crystallin domain (Ganea 2001; Stamler *et al*. 2005). In the study, α-Hsp in *H. vulgaris* was found to have two α-crystallin domains (figure 3) which share 41.18% amino acid sequence identity with each other (figure 4), and the none too high sequence identity between the two domains is probably a reflection of the complex procedure of α-Hsp evolution. In other words, at the genetic level, tandem duplications and accompanying sequence variation based on the DNA fragment encoding α-crystallin domain may have contributed significantly to the development and expansion of the *α-Hsp* gene family (Piatigorsky 2003; Augusteyn 2004).

Which one of the two functions of α-Hsp as structure protein or molecular chaperone is initial during evolution? the question is an active research topic (Schulenburg and Miller, 2014). In order to trace the evolution history of α-Hsp, in the study, a phylogenetic tree was reconstructed based on the amino-acid sequences of α-crystallin domains from different groups of animals. The phylogenetic tree showed that the α-crystallin domains of cnidaria group without eyes were the most primitive ones among these animal groups (figure 7). Due to the lack of crystalline lens in

the phylum Cnidaria, so cnidarian α-Hsp could not be structure protein, i. e., in the evolution, α-Hsp serves an original functin as molecular chaperone. And so, it is believed that α-Hsp in the vertebrate eye lens was evolutionarily recruited from chaperone protein for optical purposes, or the protein evolved with one function (as molecular chaperone) to serve a second function (as the structure protein of vertebrate eye lens) (Lee *et al*. 1993; Piatigorsky *et al*. 1994; Schulenburg and Miller, 2014). In deed, although α-Hsp in the vertebrate eye lens is structure protein, but it still retain chaperone-like properties (e. g. the ability to prevent the precipitation of denatured proteins) that are important for the maintenance of lens transparency and the prevention of cataracts (Jaenicke and Slingsby 2001).

To explore the role of α-Hsp during hydra head regeneration, qPCR analysis and whole-mount immunohistochemical assay were used for studying the expression pattern of α-Hsp during head regeneration in *H. vulgaris*. The results from immunohistochemical assay showed that α-Hsp had expressed mainly at wound site and nearby area after decapitation operation (figure 12), and both qPCR analysis and immunohistochemical assay showed that the expression of α-Hsp was up-regulated during the early regeneration period, while was down-regulated during the late regeneration period (figure 11 and 12). There are three aspects which could help us understand the role of α-Hsp during hydra regeneration. Firstly, increasing expression level of α-Hsp during the early regeneration period perhaps was the normal stress response of hydra after traumatic situations like decapitation operation which is a striking stress for organisms. Secondly, the primary events at early regeneration stages are wound healing and tissue remodeling accompanying with drastic cell activities such as dedifferentiation, apoptosis, proliferation and differentiation (Patruno *et al*. 2001; Hebb *et al*. 2006), α-Hsp maybe help keep the intracellular homeostasis in the regenerative tissue around the wound area. And finally, animal organs rely usually on protein turnover in order to regenerate its tissue (Eden *et al*. 2011; Toyama and Hetzer 2013), so the wound area of hydra may experience a massive intracellular protein turnover in the regeneration process. Protein turnover is the balance between protein synthesis and protein degradation, more synthesis than breakdown is one pre-condition of an anabolic state that builds newborn tissues for wound healing, and the molecular chaperone properties of α-Hsp could guarantee the correct foldings of a great number of newly synthesized proteins.

Moreover, in order to better understand the relationship between α-Hsp and hydra head regeneration, the effect of *α-Hsp* gene silencing on the process of hydra regeneration was researched with RNAi method in the study. The results showed that RNAi-mediated *α-Hsp* silencing led to the obvious delay of the regeneration of head structures in *H. vulgaris* (figure 14), and apparently, this phenomenon hinted an important role of *α-Hsp* gene in hydra head regeneration. Although the accurate role of *α-Hsp* gene has yet to be identified, at least, the results shown in the study indicated that this gene is functionally involved in hydra head regeneration. In conclusion, our results indicated that α-Hsp of hydra could be related with wound healing and tissue remodeling at early regeneration stages, and the physiological function and role of α-Hsp in hydra are worth further study.

Acknowledgements

This work was funded by the National Natural Science Foundation of China (no. 31171415, no. 31370406, no. 31671529).

References

Abascal F., Zardoya R. and Posada D. 2005 ProtTest: Selection of best-fit models of protein evolution. *Bioinformatics* **21**, 2104–2105.

Ali-Benali M. A., Alary R., Joudrier P. and Gautier M. F. 2005 Comparative expression of five Lea genes during wheat seed development and in response to abiotic stresses by real-time quantitative RT-PCR. *Biochim. Biophys. Acta*. **1730**, 56–65.

Andley U. 2006 Crystallins in the eye: function and pathology. *Prog. Retin. Eye Res*. **26**, 78–98.

Augusteyn R. C. 2004 alpha-crystallin: a review of its structure and function. *Clin. Exp. Optom*. **87**, 356–366.

Bienert S., Waterhouse A., de Beer T. A., Tauriello G., Studer G., Bordoli L. *et al*. 2017 The SWISS-MODEL repository-new features and functionality. *Nucleic Acids Res*. **45**, D313–D319

Birbrair A., Zhang T., Wang Z. M., Messi M. L., Enikolopov G. N., Mintz A. *et al*. 2013 Role of pericytes in skeletal muscle regeneration and fat accumulation. *Stem Cells Dev*. **22**, 2298–2314.

Bloemendal H., de Jong W, Jaenicke R., Lubsen N. H., Slingsby C. and Tardieu A. 2004 Ageing and vision: structure, stability and function of lens crystallins. *Prog. Biophys. Mol. Biol*. **86**, 407–485.

Bosch T. C. 2007 Why polyps regenerate and we don't: towards a cellular and molecular framework for hydra regeneration. *Dev Biol*. **303**, 421–433.

Bosch T. C. 2009 Hydra and the evolution of stem cells. *Bioessays* **31**, 478–486.

de Jong W. W., Caspers G. J. and Leunissen J. A. 1998 Genealogy of the alpha-crystallin-small heat-shock protein superfamily. *Int. J. Biol. Macromol*. **22**, 151–162.

Dunn S. R., Phillips W. S., Green D. R. and Weis V. M. 2007 Knockdown of actin and caspase gene expression by RNA interference in the symbiotic anemone *Aiptasia pallida*. *Biol. Bull*. **212**, 250–258.

Eden E., Geva-Zatorsky N., Issaeva I., Cohen A., Dekel E., Danon T. *et al*. 2011 Proteome half-life dynamics in living human cells. *Science* **331**, 764–768.

Egelhofer V., Gobom J., Seitz H., Giavalisco P., Lehrach H. and Nordhoff E. 2002 Protein identification by MALDI-TOF-MS peptide mapping: a new strategy. *Anal. Chem*. **74**, 1760–1771.

Galliot B. 2013 Injury-induced asymmetric cell death as a driving force for head regeneration in *Hydra*. *Dev. Genes Evol*. **223**, 39–52.

Ganea E. 2001 Chaperone-like activity of alpha-crystallin and other small heat shock proteins. *Curr. Protein. Pept. Sci*. **2**, 205–225.

Gasparov V. S. and Degtiar' V. G. 1994 Protein determination by binding with the dye Coomassie brilliant blue G-250. *Biokhimiia* **59**, 763–777.

Govindasamy N., Murthy S. and Ghanekar Y. 2014 Slow-cycling stem cells in hydra contribute to head regeneration. *Biol. Open*. **3**, 1236–1244.

Gurtner G. C., Werner S., Barrandon Y. and Longaker M. T. 2008 Wound repair and regeneration. *Nature* **453**, 314–321.

Hebb M. O., Myers T. L. and Clarke D. B. 2006 Enhanced expression of heat shock protein 27 is

correlated with axonal regeneration in mature retinal ganglion cells. *Brain Res*. **1073**, 146–150.

Hoehenwarter W., Klose J. and Jungblut P. R. 2006 Eye lens proteomics. *Amino Acids*. **30**, 369–389.

Ingolia T. D. and Craig E. A. 1982 Four small *Drosophila* heat shock proteins are related to each other and to mammalian alpha-crystallin. *Proc. Natl. Acad. Sci. USA* **79**, 2360–2364.

Jaenicke R. and Slingsby C. 2001 Lens crystallins and their microbial homologs: structure, stability, and function. *Crit. Rev. Biochem. Mol. Biol.* **36**, 435–499.

Jeon H. K., Park H., Lee D., Choe S., Sohn W. M. and Eom K. S. 2016 Molecular Detection of *Spirometra decipiens* in the United States. *Korean J. Parasitol*. **54**, 503–507.

Khalturin K., Anton-Erxleben F., Milde S., Plötz C., Wittlieb J., Hemmrich G., *et al*. 2007 Transgenic stem cells in Hydra reveal an early evolutionary origin for key elements controlling self-renewal and differentiation. *Dev. Biol*. **309**, 32–44.

Koolivand D., Bashir N. S., Behjatnia S. A. and Joozani R. J. 2016 Production of polyclonal antibody against Grapevine fanleaf virus movement protein expressed in *Escherichia coli*. *Plant Pathol. J*. **32**, 452–459.

Li Q., Yang H. and Zhong T. P. 2015 Regeneration across metazoan phylogeny: lessons from model organisms. *J. Genet. Genomics* **42**, 57–70.

Lee D. C., Gonzalez P., Rao P. V., Zigler J. S. Jr. and Wistow G. J. 1993 Carbonyl-metabolizing enzymes and their relatives recruited as structural proteins in the eye lens. *Adv. Exp. Med. Biol*. **328**, 159–168.

Lengfeld T., Watanabe H., Simakov O., Lindgens D., Gee L., Law L. *et al*. 2009 Multiple Wnts are involved in Hydra organizer formation and regeneration. *Dev. Biol*. **330**, 186–199.

MacRae T. H. 2000 Structure and function of small heat shock/alpha-crystallin proteins: established concepts and emerging ideas. *Cell. Mol. Life. Sci*. **57**, 899–913.

Naito Y., Yoshimura J., Morishita S. and Ui-Tei K. 2009 siDirect 2.0: updated software for designing functional siRNA with reduced seed-dependent off-target effect. *BMC Bioinformatics* **10**, 392.

Ninov N. and Yun M. H. 2015 Current advances in tissue repair and regeneration: the future is bright. *Regeneration (Oxf)* **2**, 84–91.

Ochiya T., Takahama Y., Baba-Toriyama H., Tsukamoto M., Yasuda Y., Kikuchi H. *et al*. 1999 Evaluation of cationic liposome suitable for gene transfer into pregnant animals. *Biochem. Biophys. Res. Commun*. **258**, 358–65.

Patruno M., Thorndyke M. C., Candia Carnevali M. D., Bonasoro F. and Beesley P. W. 2001 Growth factors, heat-shock proteins and regeneration in echinoderms. *J. Exp. Biol*. **204**, 843–848.

Petersen H. O., Höger S. K., Looso M., Lengfeld T., Kuhn A., Warnken U. *et al*. 2015 A comprehensive transcriptomic and proteomic analysis of hydra head regeneration. *Mol. Biol. Evol.* **32**, 1928–1947.

Piatigorsky J., Kantorow M., Gopal-Srivastava R. and Tomarev S. I. 1994 Recruitment of enzymes and stress proteins as lens crystallins. *EXS*. **71**, 241–250.

Piatigorsky J. 2003 Crystallin genes: specialization by changes in gene regulation may precede gene duplication. *J. Struct. Funct. Genomics* **3**, 131–137.

Poss K. D. 2010 Advances in understanding tissue regenerative capacity and mechanisms in animals. *Nat. Rev. Genet*. **11**, 710–722.

Sánchez A. A. 2000 Regeneration in the metazoans: why does it happen? *BioEssays* **22**, 578–590.

Schulenburg C. and Miller B. G. 2014 Enzyme recruitment and its role in metabolic expansion. *Biochemistry* **53**, 836–845.

Sievers F. and Higgins D. G. 2014 Clustal Omega, accurate alignment of very large numbers of sequences. *Methods Mol. Biol.* **1079**, 105–116.

Stamler R., Kappé G., Boelens W. and Slingsby C. 2005 Wrapping the alpha-crystallin domain fold in a chaperone assembly. *J. Mol. Biol.* **353**, 68–79.

Sun G. and Irvine K. D. 2014 Control of growth during regeneration. *Curr. Top Dev. Biol.* **108**, 95–120.

Toyama, B. H. and Hetzer M. W. 2013 Protein homeostasis: Live long, won't prosper. *Nature Rev. Mol. Cell Biol.* **14**, 55–61.

Valentina C., Dina A., Jianqing L., Kevin S. and Joel J. 1995 DMRIE-C reagent for transfection of suspension cells and for RNA transfections. *Focus* **17**, 84–87.

Vert J. P. , Foveau N., Lajaunie C. and Vandenbrouck Y. 2006 An accurate and interpretable model for siRNA efficacy prediction. *BMC Bioinformatics* **7**, 520.

Wenger Y., Buzgariu W., Reiter S. and Galliot B. 2014 Injury-induced immune responses in *Hydra*. Semin. Immunol. **26**, 277–294.

White J. J. and Sillitoe R. V. 2013 Postnatal development of cerebellar zones revealed by neurofilament heavy chain protein expression. *Front Neuroanat.* **7**, 1–10.

Yun M. H. 2015 Changes in regenerative capacity through lifespan. *Int. J. Mol. Sci.* **16**, 25392–25432.

Received 31 October 2017; revised 6 December 2017; accepted 30 January 2018

Table 1. PCR primers used in the study.

Usage	Primer code	Sequence (5'-3')	Source of primers
RACE	5' Hsp	GTCTATCATTAAACAGTGGAG	This study
	3' Hsp	AGAAGTTTCTCTTAAAGTAGAAGGAC	This study
	5' adapter primer	AGCAGTGGTATCAACGCAGAGT	SMART RACE cDNA Amplification Kit
	3' adapter primer	TTCTAGAGGCCGAGGCGGCC	SMART RACE cDNA Amplification Kit
	Hsp-F	CTGCTTAATTTTACGATTATAGCAC	This study
	Hsp-R	TCTGATGCAAAATAAGTTAC	This study
prokaryotic	PE-Hsp-F	CAGCACCATGGGCTCTTTATGGCATGTACCTGTCCATGA	This study
expression	PE-Hsp-R	AGTATCTCGAGTTCTTCCATTTTGACCTCAAGTTTGAGT	This study
qPCR	Q-Hsp-F	CATGATCGTCTATACAGAGAT	This study
	Q-Hsp-R	ATTGCGATTGGATCAACATCA	This study
	Q-Actin-F	TCAGACAAATGAATTGTCCATG	This study
	Q-Actin-R	TCCAATGTATCATGTAACGT	This study

Table 2. Five candidate siRNA sequences designed for RNAi-mediated *α-Hsp* gene silencing in *H. vulgaris*.

siRNA name	Target position in the coding region	Sense sequence (5'-3')	Antisense sequence (5'-3')
Hsp-siRNA-1	250-272	AGAAGAAGUUUCUCUUAAAGU	UUUAAGAGAAACUUCUUCUGG
Hsp-siRNA-2	383-405	GCAAUUACUUCUAAUAUUAGU	UAAUAUUAGAAGUAAUUGCGA
Hsp-siRNA-3	517-539	AGAGGAAAUUUCAAUUCAAGU	UUGAAUUGAAAUUUCCUCUGG
Hsp-siRNA-4	535-557	AGUUAAAGGUAGAGAUUUAGU	UAAAUCUCUACCUUUAACUUG
Hsp-siRNA-5	616-638	GCAGUUUACUCGAAACAUAUC	UAUGUUUCGAGUAAACUGCUU